Static and dynamic magnetic properties of epitaxial Co_2FeAl Heusler alloy thin films

G. Ortiz,[1,2,a)] M. S. Gabor,[3,4] T. Petrisor, Jr.,[4] F. Boust,[2] F. Issac,[2] C. Tiusan,[3] M. Hehn,[3] and J. F. Bobo[1,5]
[1]*NMH-CEMES, CNRS, Toulouse, France*
[2]*ONERA, Toulouse, France*
[3]*Institut Jean Lamour, P2M, CNRS-Nancy University, Nancy, France*
[4]*Technical University of Cluj Napoca, Materials Science Laboratory, Cluj, Romania*
[5]*GLAM - MSE Department, Stanford University, Stanford, California 94305, USA*

(Presented 16 November 2010; received 27 September 2010; accepted 12 November 2010; published online 30 March 2011)

Structural and magnetic properties of epitaxial Co_2FeAl Heusler alloy thin films were investigated. Films were deposited on single crystal MgO (001) substrates at room temperature, followed by an annealing process at 600 °C. MgO and Cr buffer layers were introduced in order to enhance crystalline quality, and improve magnetic properties. Structural analyses indicate that samples have grown in the *B*2 ordered epitaxial structure. VSM measures show that the MgO buffered sample displays a magnetization saturation of 1010 ± 30 emu/cm^3, and Cr buffered sample displays a magnetization saturation of 1032 ± 40 emu/cm^3. Damping factor was studied by strip-line ferromagnetic resonance measures. We observed a maximum value for the MgO buffered sample of about 8.5×10^{-3}, and a minimum value of 3.8×10^{-3} for the Cr buffered one. © *2011 American Institute of Physics*. [doi:10.1063/1.3549581]

I. INTRODUCTION

Heusler alloy thin films have recently gained great interest as electrodes for magnetic tunnel junctions,[1,2] and as low damping magnetic materials for rf applications.[3] Heusler alloys are usually separated in two different categories: half-Heusler and full-Heusler. The first is described by the formula XYZ and the second by X_2YZ, where X and Y are transition metal atoms like Co, Fe, Ni, and Z is a main-group sp-atom like Al, Si, Ge, Sb. Half-Heuslers crystallize in $C1_b$ structure, while full-Heuslers crystallize in $L2_1$, *B*2, or *A*2, structures. $C1_b$ structure presents vacancies in lattice sites, while in $L2_1$ structure, these vacancies are occupied by X atoms. The *B*2 structure presents a (Y,Z) site disorder, while the *A*2 structure involves a totally (X,Y,Z) site disorder relative to the perfectly ordered $L2_1$ structure. It has been predicted that Co-based full-Heusler alloys behave like half–metals[4–6] (100% spin polarized at Fermi level) even at room temperature, allowing huge tunnel magnetoresistance. Among Co-based full-Heusler alloys, Co_2FeAl (CFA) is a very attractive material because it allows giant tunneling magnetoresistance up to 330% (Ref. 7) and has low damping.[8] The latter, is an important parameter because it is tightly related to the material's dynamic time of response,[9] and thereby, fundamental for high speed devices applications.

In this work we have studied the relation between structural and magnetic properties of two CFA films epitaxilly grown on MgO substrates.

II. EXPERIMENT AND MEASUREMENT

The films were grown on MgO (001) single crystal substrates using rf magnetron sputtering in a system having a base pressure of 3×10^{-8} Torr. Prior to deposition, the MgO (001) substrates were heated up to 700 °C for 30 min in vacuum. After cooling down to room temperature (RT), a 10-nm-thick MgO or 15-nm-thick Cr buffer layer was deposited on the substrate. The MgO buffer layer was grown by rf sputtering using a MgO polycrystalline target, under an Ar pressure of 5.0 mTorr, while the Cr buffer was deposited by dc sputtering, at an Ar pressure of 1.0 mTorr. After the buffer layer deposition, a 55-nm-thick Co_2FeAl film was deposited by rf sputtering from a stoichiometric target ($Co_{50\%}Fe_{25\%}Al_{25\%}$). The Ar pressure during sputtering was kept at 1.0 mTorr and the typical deposition rate was 1.5×10^{-2} nm/s. Subsequently, in order to improve the crystalline quality, the samples were transferred into an UHV chamber (base pressure better than 10^{-10} Torr) and reflection high-energy electron diffraction (RHEED) assisted annealed for 15 min at 600 °C. After cooling down to room temperature (RT) a 10-nm-thick Au capping layer was deposited by e-beam evaporation. The structural properties were examined by RHEED and x-ray diffraction (XRD) using a high-resolution four circles diffractometer (Bruker AXS).

The static magnetic properties were studied by vibrating sample magnetometry (VSM) and dynamic magnetic properties by strip-line ferromagnetic resonance (FMR) in an in-plane configuration. In the latter, the applied field H_{ext} was along an easy axis and the rf field h_{rf}, perpendicular to that axis. Samples were studied between 6 and 26.5 GHz.

III. RESULTS

Figure 1 shows the RHEED patterns, for the Cr and MgO buffered CFA films, along the azimuth [110]MgO (corresponding to [100]CFA) obtained after annealing the

a)Electronic mail: guillermo.ortiz@onera.fr.

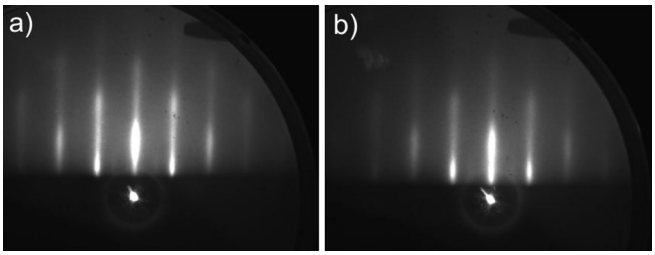

FIG. 1. RHEED patterns, along the azimuth [110]MgO (corresponding to [100]CFA) obtained for the (a) Cr buffered and (b) MgO buffered CFA films after annealing the samples at 600 °C.

samples at 600 °C for 15 min. The streak patterns confirm the epitaxial growth of CFA films according to the CFA(001) [110] || MgO(001) [100] epitaxial relation. Figure 2 shows the X-ray θ–2θ (out-of-plane) diffraction patterns for MgO and Cr buffered CFA films, after annealing. In addition to the peak corresponding to the MgO substrate, the films exhibit only the (002), (004)CFA, and (002)Cr peaks. The presence of (002)CFA reflection suggests that the films are in $B2$ structure. The perfectly ordered $L2_1$ structure is characterized by the presence of superlattice reflections like (111) or (311). In order to prove the presence or absence of superlattice peaks we performed in-plane φ-scan measurements. No $L2_1$ (111) reflection could be observed, which implies the presence of $B2$ structure, characterized by total disorder between Fe and Al, while Co atoms occupy regular sites.

The in-plane ($a_{\parallel}$) and out-of-plane ($a_{\perp}$) CFA films' lattice parameters were determined by scanning the reciprocal lattice, where h, k and l are the usual Miller coordinates. First we performed an l-scan (θ–2θ symmetrical geometry) around the 002 node of the CFA reciprocal lattice and obtained the d_{002} distance which allows us to derive $a_{\perp}$. Using the l coordinate we performed an $h=k$ scan (θ–2θ asymmetrical geometry) around 224 CFA reciprocal lattice node and obtained d_{224} distance, which we use to derive $a_{\parallel}$. The as obtained values are $a_{\perp} = 0.5726 \pm 0.0001$ nm and $a_{\parallel} = 0.5729 \pm 0.0001$ nm for the MgO buffered film and $a_{\perp} = 0.5735 \pm 0.0001$ nm and $a_{\parallel} = 0.5722 \pm 0.0005$ nm for the Cr buffered one. The results indicate that the CFA lattice constants are relaxed for both films and have a value very close to the bulk one [0.573 nm (Ref. 10)].

The intensities (I_P) of the (002) and (004) peaks for the Cr buffered sample are larger than for the MgO buffered one, indicating better crystallinity for Cr buffered film, also suggested by the RHEED patterns, and it most likely due to the smaller lattice misfit (−0.65%) between CFA (001) and Cr (001) than between CFA(001) and MgO(001) on 45° in-plane rotation (−3.92%). In order to extract I_P (004) value for the Cr buffered film we have fitted the overlapping (002) Cr and (004) CFA peaks with two pseudo-Voight functions keeping the (004) CFA peak position fixed to the value calculated from the (002) CFA peak position.

The (002) reflection is characteristic of the $B2$ structure, and thus the peaks intensity ratio $I_P(002)/I_P(004)$ is a measure of the degree of order on Co sites. This ratio is almost identical for both samples, suggesting the same degree of $B2$ ordering regardless of the buffer layer.

The static magnetic properties of the epitaxial CFA films were investigated by VSM at RT. Figure 3 shows normalized magnetization versus applied magnetic field for magnetic fields applied in-plane along the [100] and [110] crystallographic directions of the CFA film. An in-plane anisotropy is observed in both Cr [Fig. 3(a)] and MgO [Fig. 3(b)] buffered films. The magnetic easy axis is along [110] direction, while the hard axis lies along [100] direction. The saturation magnetization M_s value was 1010 ± 30 emu/cm^3 for MgO buffered sample and 1032 ± 40 emu/cm^3 for Cr buffered one.

Dynamics of magnetization were studied by strip-line FMR. In order to evaluate the frequency dependence of resonance field position (H_r) and linewidth (ΔH), we performed measures between 6 and 26.5 GHz in an in-plane configuration with the external field along the easy-axis. Figure 4 shows H_r as a function of frequency. The curves were fitted using the well-known Kittel's formula[11] for the current

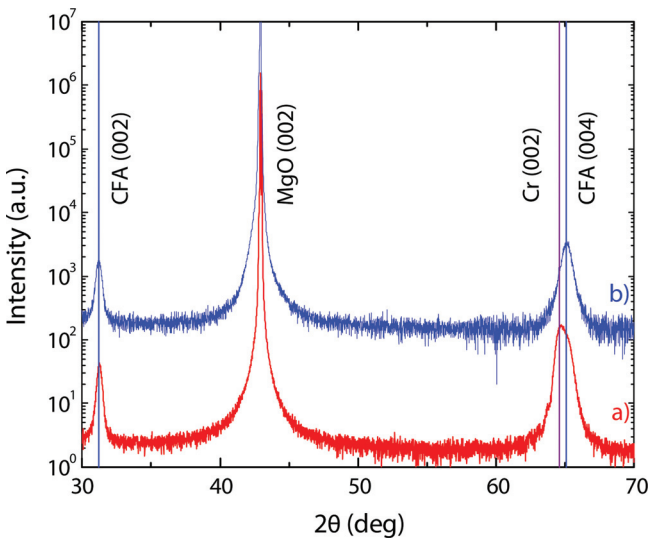

FIG. 2. (Color online) XRD out-of-plane pattern for the (a) Cr buffered and (b) MgO buffered CFA films after annealing at 600 °C. The vertical lines indicate the CFA(002), CFA(004), and Cr(002) bulk peak positions.

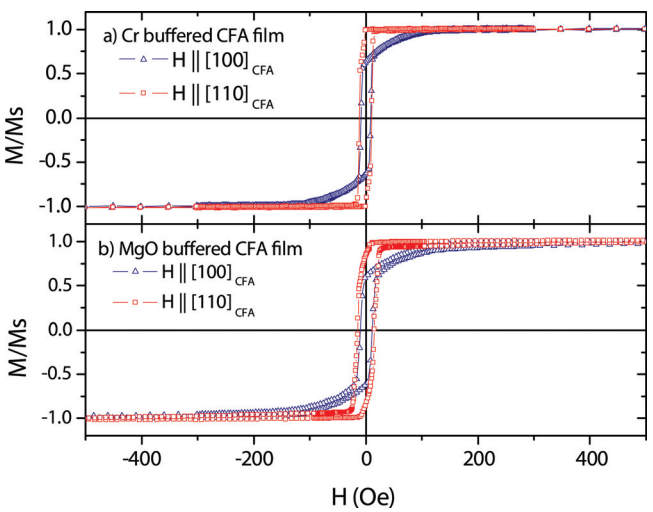

FIG. 3. (Color online) Magnetic hysteresis loops for the (a) Cr buffered and (b) MgO buffered CFA films. Measurements were carried out at RT with the magnetic field applied in the film plane along [100] and [110] CFA, respectively.

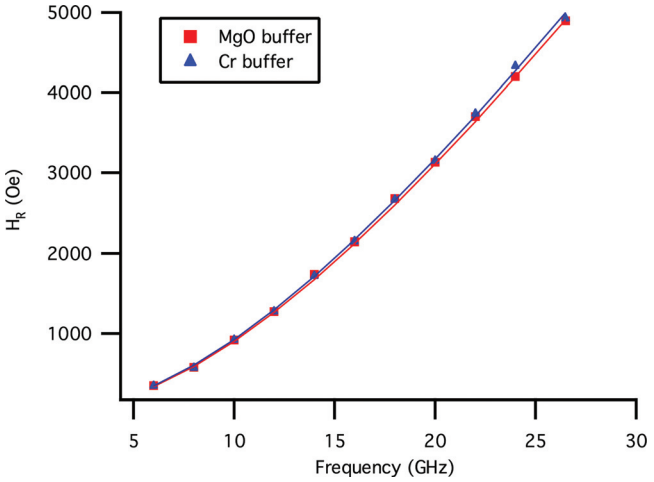

FIG. 4. (Color online) Resonance field H_r as a function of frequency for Cr and MgO buffered samples.

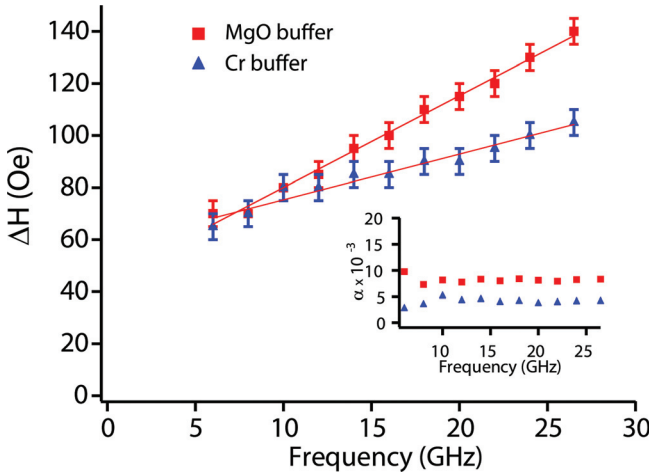

FIG. 5. (Color online) Frequency dependence of linewidth ΔH. The inset shows α as a function of frequency.

configuration, where we neglected anisotropy (having a low influence especially at high frequencies):

$$\omega = \gamma\sqrt{H_r(H_r + 4\pi M_s)}. \quad (1)$$

γ is the gyromagnetic ratio, defined as $\gamma = g(\mu_B/\hbar)$, and M_s is saturation magnetization. The solid lines in Fig. 4 represent fitting results using Eq. (1) and the samples' M_s values. The adjustment parameter was the gyromagnetic ratio γ. We estimated the value of g to be 2.02 ± 0.02 for both samples. Figure 5 shows linewidth ΔH as a function of frequency. We note the intersection between the curve and the Y axis as the extrinsic linewidth ΔH_0, which reflects the sample's inhomogeneities.[12,13] We found a ΔH_0 of about 45 Oe for MgO buffered sample, and 58 Oe for the Cr buffered one. It appears that the presence of inhomogeneities is larger for the Cr buffered sample.

Linewidth is an important parameter because it allows one to calculate the materials damping factor α with[14]:

$$\Delta H = \frac{2}{\sqrt{3}}\frac{\alpha\omega}{\gamma} + \Delta H_0. \quad (2)$$

the inset to Fig. 5 shows the frequency dependence of α for both samples. Damping factor remains constant in the frequency range studied. Measurements yielded an average damping factor value of 8.5×10^{-3} for the MgO buffered sample, and of 3.8×10^{-3} for the Cr buffered one.

IV. CONCLUSION

In this paper we reported a structural and magnetic study of two Co_2FeAl samples; one with MgO buffer and the other with Cr buffer. RHEED and XRD demonstrated that both samples were epitaxially grown in the $B2$ phase. It appears that Cr buffer provides a better crystalline quality, as evidenced by XRD, larger saturation magnetization, and lower damping factor. However this sample presents a larger extrinsic linewidth, indicating the presence of more inhomogeneities than for the MgO buffered one.

This work has been partially supported by CNCSIS UEFISCSU, project number PNII IDEI No.4/2010, code ID-106 and by POS CCE ID. 574, code SMIS-CSNR 12467.

[1]S. Kammerer, A. Thomas, A. Hutten, and G. Reiss, Appl. Phys. Lett. **85**, 79 (2004).
[2]S. Tsunegi, Y. Sakuraba, M. Oogane, K. Takanashi, and Y. Ando, Appl. Phys. Lett. **93**, 112506 (2008).
[3]B. Rejaei and M. Vroubel, J. Appl. Phys. **96**, 6863 (2004).
[4]S. Ishida, S. Fujii, S. Kashiwagi, and S. Asano, J. Phys. Soc. Jpn. **64**, 2152 (1995).
[5]I. Galanakis, P. H. Dederichs, and N. Papanikolaou, Phys. Rev. B **66**, 174429 (2002).
[6]S. Picozzi, A. Continenza, and A. J. Freeman, Phys. Rev. B **66**, 094421 (2002).
[7]W. Wang, H. Sukegawa, R. Shan, S. Mitani, and K. Inomata, Appl. Phys. Lett. **95**, 182502 (2009).
[8]S. Mizukami, D. Watanabe, M. Oogane, Y. Ando, Y. Miura, M. Shirai, and T. Miyazaki, J. Appl. Phys. **105**, 07D306 (2009).
[9]R.l Yilgin, Y. Sakuraba, M. Oogane, S. Mizukami, Y. Ando, and T. Miyazaki, Jpn. J. Appl. Phys. 46, L205 (2007).
[10]Ziebeck, Webster, and Landolt-Bornstein, New Series III/19c (Springer, Berlin, 1988).
[11]C. Kittel, Phys. Rev.**73**, 155 (1948).
[12]D. J. Twisselmann and R. D. McMichael, J. Appl. Phys. **93**, 6903 (2003).
[13]Z. Celinski and B. Heinrich, J. Appl. Phys.**70**, 5935 (1991).
[14]C.E. Patton, J. Appl. Phys. **39**, 3060 (1968).